Vol 17 No 4, January 2008
1674-1056/2008/17(04)/1364-07

Chinese Physics B

© 2008 Chin. Phys. Soc.
and IOP Publishing Ltd

First-principles local density approximation (LDA) + U and generalized gradient approximation (GGA) + U studies of plutonium oxides*

Sun Bo(孙 博) and Zhang Ping(张 平)†

Institute of Applied Physics and Computational Mathematics, Beijing 100088, *China*

(Received 10 September 2007; revised manuscript received 10 October 2007)

The electronic structures and properties of PuO_2 and Pu_2O_3 have been studied according to the first principles by using the all-electron projector-augmented-wave (PAW) method. The local density approximation (LDA)+U and the generalized gradient approximation (GGA)+U formalisms have been used to account for the strong on-site Coulomb repulsion among the localized Pu 5f electrons. We discuss how the properties of PuO_2 and Pu_2O_3 are affected by choosing the values of U and exchange-correlation potential. Also, the oxidation reaction of Pu_2O_3, leading to the formation of PuO_2, and its dependence on U and exchange-correlation potential have been studied. Our results show that by choosing an appropriate U it is possible to consistently describe structural, electronic, and thermodynamic properties of PuO_2 and Pu_2O_3, which enable the modelling of the redox process involving Pu-based materials.

Keywords: the first-principles calculation, LDA + U, GGA + U, plutonium oxides
PACC: 7115A,7115H, 7115M, 7125

1. Introduction

Plutonium dioxide (PuO_2) and sesquioxide (Pu_2O_3) are the only observed stoichiometric compounds formed at the surface of the metallic plutonium when exposed to dry air[1] (nonstoichiometric oxide may form by reaction of dioxide with water[2]). In this sense, plutonium corrosion and oxidation are often treated as an equivalent topic. The plutonium corrosion plays a key role in considering the nuclear stockpile and storage of surplus plutonium. Therefore, a thorough understanding of the physical and the chemical properties of the plutonium oxide is always needed.

From the view point of basic research, it can be visualized that many physical and chemical properties of the plutonium oxide are closely related to the quantum processes of localization and delocalization for Pu 5f electrons. The modelling of the electron localization, and thus any redox process involving plutonium, is a complex task. Conventional density functional schemes, in which the local density approximation (LDA) or the generalized gradient approximation (GGA) is adopted, underestimate the strong on-site Coulomb repulsion of the Pu 5f electrons and consequently fail to capture the correlation-driven localization. Therefore, the 5f electrons in elemental Pu, as well as in Pu compounds, require special attention. One promising way to improve contemporary LDA and GGA approaches is to modify the intra-atomic Coulomb interaction through the so-called LDA+U or GGA+U approach, in which the underestimation of the intraband Coulomb interaction is corrected by the Hubbard U parameter.[3−5] In short, DFT+U correction acts as reducing the one-electron potential locally for the specified orbitals of the respective atoms (e.g. Pu 5f orbitals), therefore reducing the hybridization with orbitals of the ligands (e.g. O atoms). This method has been used to discuss the equilibrium lattice parameter of bulk Pu in Ref.[6]. The choice of U is not unambiguous, but it is not trivial to determine its value a priori, though there are attempts to extract it from standard first-principles calculations. Hence, U is often fitted to reproduce a certain set of experimental data such as band gaps and structural properties.

As the density-functional theory (DFT) is powerful to be applied in a wide range of scientific researches,[7−21] and motivated by the recent suc-

*Project supported by the National Natural Science Foundation of China (Grant No 10604010).
†Corresponding author. E-mail: zhang_ping@iapcm.ac.cn

cessful calculations on 4f cerium oxide within the DFT+U formalism,[22,23] in this paper we use the LDA+U and GGA+U schemes formulated by Dudarev *et al*[24] to calculate the lattice parameters, thermodynamic properties, and band structures of PuO_2 and Pu_2O_3. We discuss how these properties are affected by the choice of U as well as the choice of exchange-correlation potential, i.e. the LDA or the GGA, and how redox processes occurring in plutonium oxide can be described by using the LDA+U and GGA+U formalisms.

This paper is organized as follows. The details of our calculations are described in Section 2 and in Section 3 we present and discuss the results. In Section 4, we summarize our findings.

2. Methodology of the calculation

The calculations were performed using the projector-augmented wave (PAW) method of Blöchl,[25] as implemented in the ab initio total-energy and molecular-dynamics program VASP (Vienna ab initio simulation program).[26−29] The PAW is an all-electron method that combines the accuracy of augmented-plane-wave methods with the efficiency of the pseudopotential approach. The PAW method is implemented in VASP in the frozen-core approximation. For a plane-wave set, a cut-off energy of 400 eV was used. The plutonium 6s, 6p, 7s, and 5f, and the oxygen 2s and 2p electrons were treated as valence electrons. We used the LDA+U formalism formulated by Dudarev *et al*[24] to account for the strong on-site Coulomb repulsion amongst the localized Pu 5f electrons. In this scheme the total LDA (GGA) energy functional is of the form

$$E_{\mathrm{LDA(GGA)}+U} = E_{\mathrm{LDA(GGA)}} + \frac{U-J}{2}\sum_{\sigma}\left[\mathrm{Tr}\rho^{\sigma} - \mathrm{Tr}\left(\rho^{\sigma}\rho^{\sigma}\right)\right], \quad (1)$$

where ρ^{σ} is the density matrix of f states, and U and J are the spherically averaged screened Coulomb energy and the exchange energy, respectively. Here only the difference between U and J is significant[24] and consequently we henceforth treated them as one single parameter, for simplicity labelled as U.

The exchange and the correlation effects were treated in both the local density approximation and the generalized gradient approximation.[30] We studied PuO_2 in its ground-state fluorite structure ($Fm3m$) and the sesquioxide Pu_2O_3 in the hexagonal A-type structure ($P\bar{3}m1$). For PuO_2 we used a $11\times11\times11$ Monkhorst-Pack k-point mesh[31] (56 irreducible k points) and for Pu_2O_3 we used a $9\times9\times6$ grid (57 irreducible k points). The electronic density of state (DOS) was obtained with $15\times15\times15$ (120 irreducible k points) and $11\times11\times9$ grid (120 irreducible k points) k-point meshes, separately. The Brillouin-zone integration was performed using the modified tetrahedron method given by Blöchl *et al.*[32] In order to study the reaction energy it is necessary to calculate the energy of an oxygen molecule (E_{O_2}). The effect of spin polarization was included in calculating E_{O_2}.

3. Results and discussion

3.1. Atomic and electronic structures of PuO_2

PuO_2 is an insulator featuring cubic $Fm3m$ structure of CaF_2 (Fig.1(a)) with the experimentally determined lattice parameter $a_0 = 0.5396$ nm at 25°C.[33] The present calculated a_0 and bulk modulus B of PuO_2 were obtained by minimizing the corresponding energy at constant volumes and by fitting a Birch–Murnaghan equation of state to the resulting energy-volume data,[34,35] respectively. The calculated energy-volume data for a series of values of U within the LDA and the GGA schemes are shown in Figs.2(a) and (b), respectively. After the fitting of the data in Fig.2 by a Birch–Murnaghan equation of state, the derived lattice parameter a_0 and the bulk modulus B as a function of U are shown in Figs.3(a) and (b), respectively. The experimental value of a_0 is also shown in Fig.3(a). It can be seen from Fig.3(a) that the relation between a_0 and U does not follow a simple monotonically linear function for both the LDA and the GGA. At small values of U ($\leqslant$1 eV), the change in lattice parameter is somewhat insensitive to the variation of U, and both the LDA and the GGA underestimate the lattice parameter. This feature rarely occurs in the usual DFT calculations. In most cases, the LDA generally underestimates the lattice parameter while the GGA often gives a slight overestimate. When U is increased to 1 eV, then a_0 starts to rapidly go up with U. The next turning point is at $U = 3$ eV, away from which the increase of a_0 starts to slow down with

U. This feature that the values of a_0 increases as a function of U is almost the same for the LDA and the GGA. The experimental result[33] of $a_0 = 0.5396\,\text{nm}$ is well fitted at $U = 3\,\text{eV}$ for the GGA, while the LDA always underestimates a_0 by at least 0.006 nm. It shows from Fig.3(b) that the calculated bulk modulus B varies with U over a rather broad range from 180 to 205 GPa for the GGA and from 200 to 230 GPa for the LDA. In particular, the GGA at $U = 3\,\text{eV}$ gives a bulk modulus $B \approx 200\,\text{GPa}$. At present there are no experimental data of bulk modulus available for PuO_2. Thus our calculated result of B needs to be verified in the future. Note that the calculation of the bulk modulus by using the stress tensor, i.e. a pressure versus volume fit instead of energy versus volume fit we referred so far, gave a slightly lower bulk modulus due to the so-called Pulay stress which arises from incompleteness of the plane wave basis set with respect to the change in volume.[36] It follows (see Fig.3(a)) that the GGA is in better agreement with the experiment than the LDA.

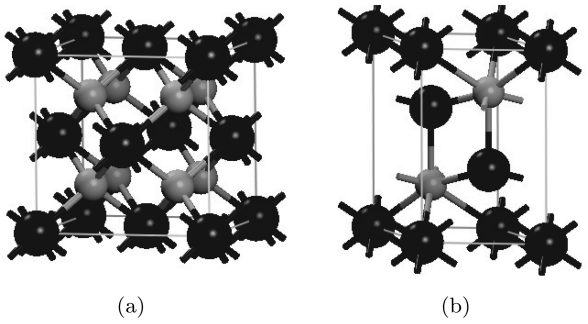


Fig.1. Fluorite-type structure of PuO_2 (a) and the sesquioxide A-type structure of Pu_2O_3 (b), where the large black and the small grey balls indicate Pu and O atoms, respectively.

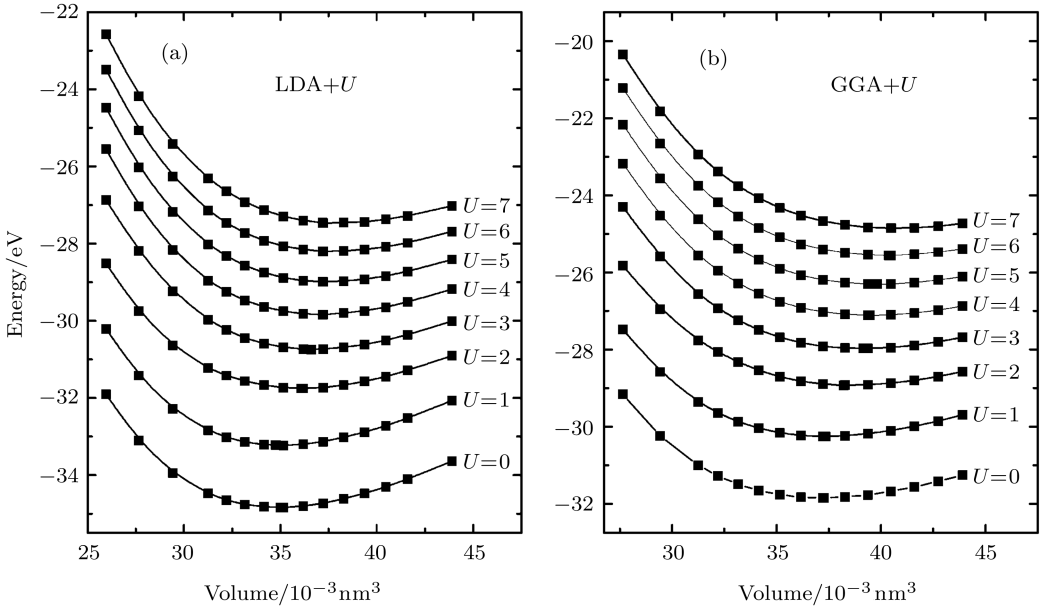


Fig.2. The LDA total energy versus the volume of unit cell of PuO_2 for several values of U (a) and the GGA total energy versus the volume of unit cell of PuO_2 for several values of U (b).

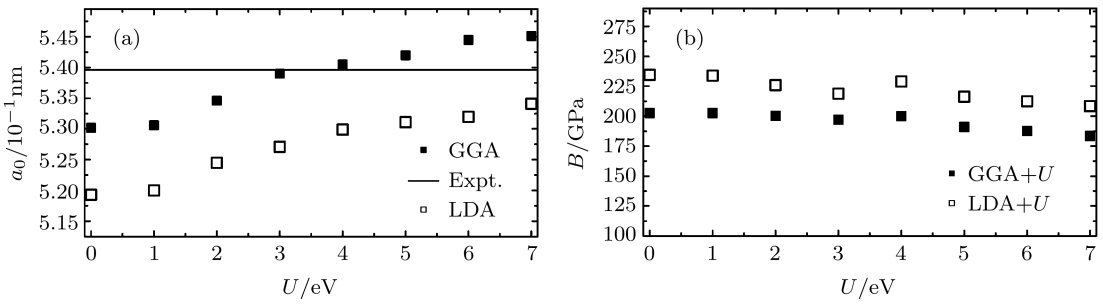


Fig.3. Dependences of the lattice parameter (a) and bulk modulus (b) of PuO_2 on U.

The structural features in Fig.3 are closely related to the electronic structure of PuO_2. In Fig.4(a) we plot the LDA site-projected partial DOS for PuO_2 for two chosen values of U, i.e. $U = 0$ (upper panel) and $U = 3$ eV (lower panel). The GGA results of the DOS are shown in Fig.4(b). The Fermi energy E_F has been set to be zero. Without accounting for Coulomb repulsion ($U = 0$), one can see that both the LDA and the GGA predict an incorrect metallic ground state for PuO_2, i.e. non-zero occupations of Pu 5f states at E_F. Switching on U, as shown in Fig.4, the Pu 5f band starts to split at E_F and tends to open a gap for both the LDA and the GGA. The amplitude of the gap increases with U increasing (see the inset in Fig.4). A prominent distinction between the LDA and the GGA results in Fig.4 is that at $U = 3$ eV the GGA

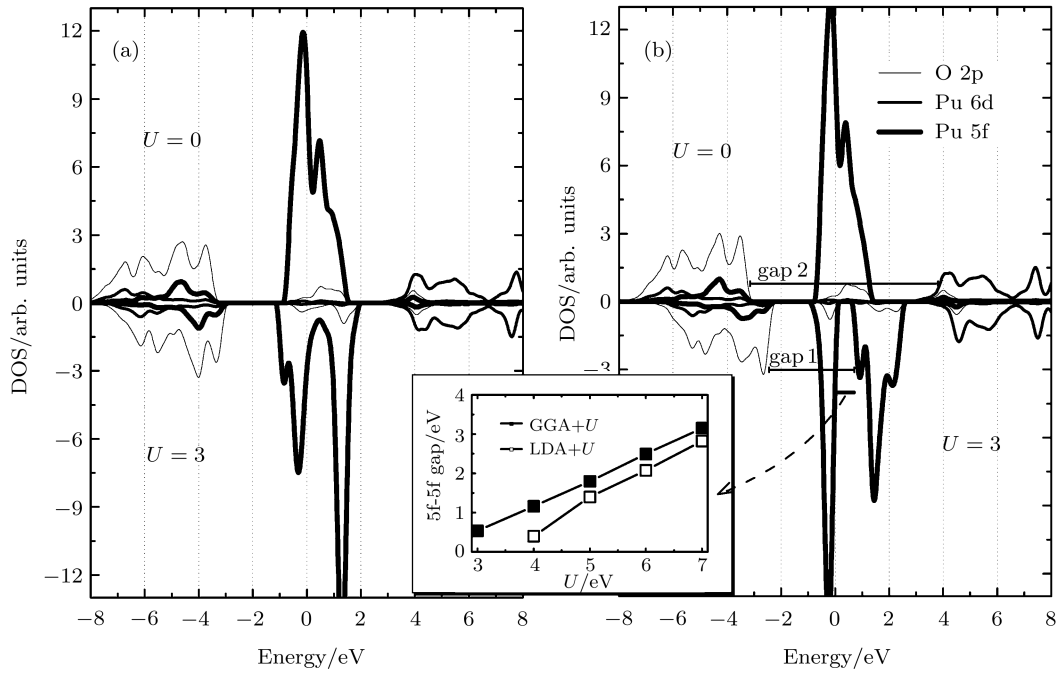


Fig.4. The LDA site-projected partial densities of state of PuO_2 (a) and the GGA results (b) for $U = 0$ (upper panel) and $U = 3$ eV (lower panel). The inset shows the band splittings of the Pu 5f states as a function of U for the LDA (open squares) and GGA (solid squares), respectively.

already predicts the correct insulating ground state of PuO_2. It is in accord with the structural prediction in Fig.3 that the GGA with $U = 3$ eV produces the lattice parameter in good agreement with the experimental result. On the other hand, however, the LDA with $U = 3$ eV still predicts a metallic ground state of PuO_2, since the gap only partially opens at this value of U. We notice that the splitting gap of Pu(5f) band calculated using the GGA is always more prominent than using the LDA (see the inset in Fig.4). Therefore, as from Fig.3, one can conclude from Fig.4 that compared with the LDA+U, the GGA+U gives more reliable prediction on the ground state of PuO_2. Additional important features in the DOS are the gaps between O(2p) valence band and Pu(5f) conduction band, and between O(2p) valence band and Pu(6d) conduction band. These gaps can be experimentally measured by high-energy spectroscopies. Figure 5 displays these two gaps as a function of U. It can be seen that the O(2p)-Pu(5f) gap changes more prominently than the O(2p)-Pu(5f) gap with U increasing. The

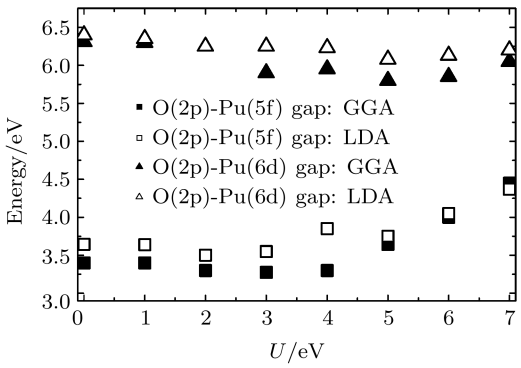


Fig.5. Dependences of O(2p)-Pu(5f) and O(2p)-Pu(6d) band gaps on U for PuO_2.

latter remains almost invariant in a wide range of U, while the former steadily increases with U increasing, which reflects the imposition of 5f electron localization by the Coulomb interaction.

3.2. Atomic and electronic structures of Pu_2O_3

Pu_2O_3 is an insulating oxide of the hexagonal sesquioxide A-type ($P\bar{3}m1$) (Fig.1(b)). At present no experimental data of structural parameters of Pu_2O_3 are available. Inspired by the above agreement of the calculated lattice parameter of PuO_2 with the experimental result, however, we expect that a systematic first-principles study of Pu_2O_3 in terms of U is also useful for the future experimental reference.

The calculated equilibrium lattice parameter a_0 of Pu_2O_3 as a function of U is plotted in Fig.6(a). As shown in the case of PuO_2, the relation between a_0 and U does not follow a simple monotonic function. Again, the curvature of a_0 curve for small values of U is more significant than for large values of U. The turning point is at $U = 3$ eV with the GGA lattice parameter $a_0 = 0.376$ nm. The decrease in curvature at large values of U corresponds to the separation of the occupied Pu 5f band from the unoccupied part, i.e. the transition from a metallic to an insulating ground state of Pu_2O_3 (see below). The equilibrium volume of the Pu_2O_3 unit cell (including 5 atoms) as a function of U is plotted in Fig.6(b). Again, the different curvatures of the volume curve for small and large values of U can be clearly seen. Overall, the effect of U is similar to what is found for PuO_2, but, and a crucial point is that the observables of Pu_2O_3 are much more affected by variation of U than those of PuO_2. With U increasing from 0 to 7 eV, the lattice constant of Pu_2O_3 varies over a range of 0.02 nm, compared with the corresponding variations of 0.01 nm for PuO_2. These data clearly demonstrate that the ground state properties of Pu_2O_3 are considerably more sensitive to the choice of U.

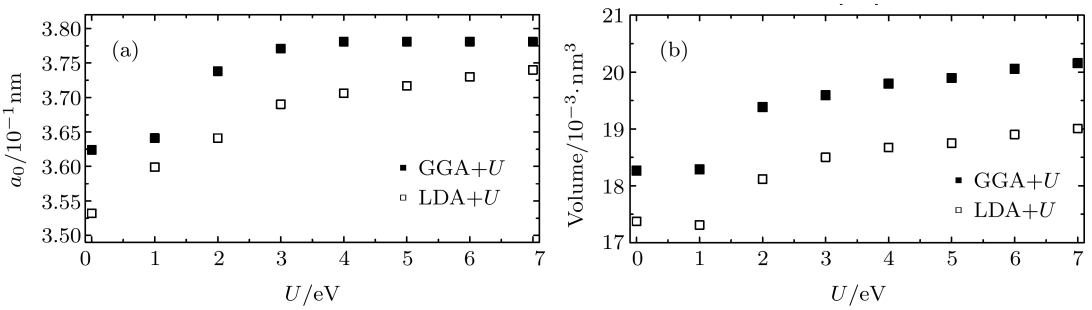


Fig.6. Dependences of the equilibrium lattice parameter a_0 (a) and the volume of unit cell (b) of Pu_2O_3 on U.

The LDA and GGA electronic DOSs for Pu_2O_3 for two chosen values of U are shown in Fig.7. Both the LDA and GGA each predict a metallic ground state for Pu_2O_3 at $U = 0$, i.e. the presence of non-zero occupation of Pu 5f state at the Fermi energy E_F. Turning on the on-site Coulomb repulsion, the Pu 5f band starts to split at and below E_F for both the LDA and the GGA. As a result, two gaps form with their amplitudes increasing with U. This is different from the case of PuO_2, in which only one gap occurs at the Fermi level. Thus the Coulomb repulsion effect on Pu 5f electronic structure is even more prominent for Pu_2O_3, and as a result, the electronic distribution will be qualitatively changed. Compared with the LDA, the GGA gives a more reliable electronic structure, since the GGA gap at E_F is clearer in most of a range of U, while the LDA gives some edge states at E_F even for large values of U. This can also be seen from the inset in Fig.7, which plots the Pu(5f)-Pu(5f) gap at E_F as a function of U, and shows the larger gap for the GGA than for the LDA.

Figure 8 displays the LDA and the GGA energy distance between the O(2p) band and the bottom of the Pu(5f) valence band (i.e. gap 1 labelled in Fig.7(b)), as well as the distance between the O(2p) band and the Pu(5f) empty band (i.e. gap 2 labelled in Fig.7(b)), as a function of U. It can be seen that the two distances change very little for small values of U. When $U \geq 1$ eV, then the former distance steadily curves down and tends to zero with U increasing, while the latter distance slowly goes up, which reflects the enhancement of 5f electron localization by the effective Coulomb repulsion.

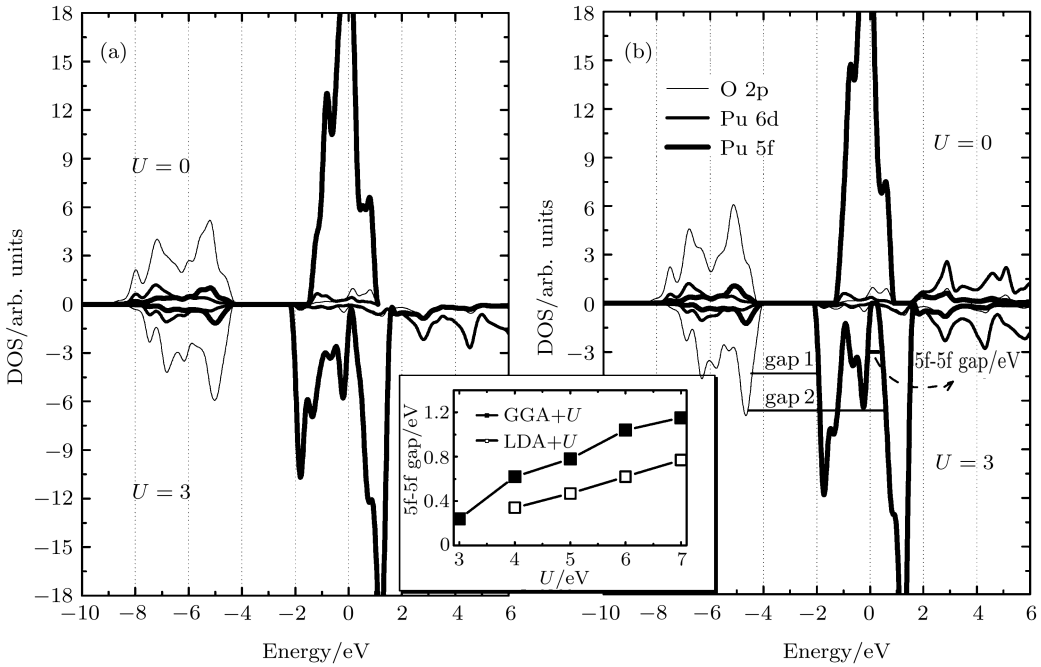


Fig.7. The LDA site-projected partial densities of state of Pu_2O_3 for $U = 0$ (upper panel) and $U = 3\,\mathrm{eV}$ (lower panel) (a) and the GGA results (b), where the inset shows the band splitting of the Pu 5f state as a function of U for the LDA (open squares) and GGA (solid squares), respectively.

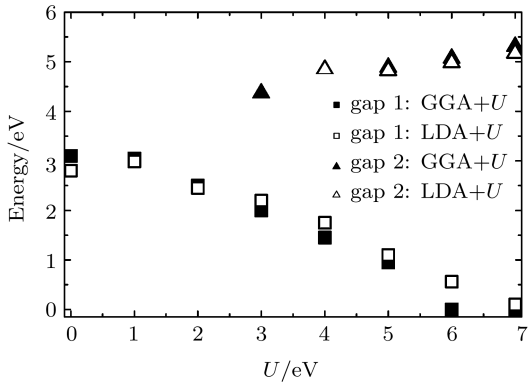


Fig.8. Dependences of band gaps on U between O(2p) and occupied Pu(5f) states, and between O(2p) and unoccupied Pu(5f) states for Pu_2O_3.

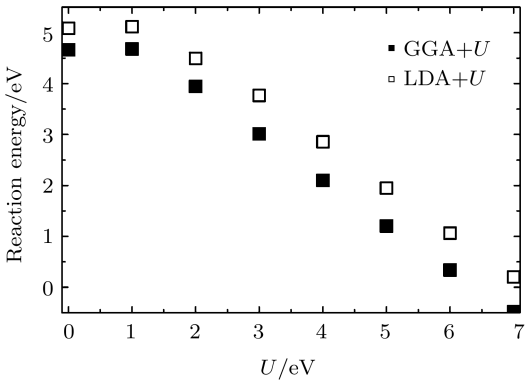


Fig.9. Dependences of the $Pu_2O_3 + \frac{1}{2}O_2 \rightarrow PuO_2$ reaction energy on U for the GGA+U (solid squares) and the LDA+U (open squares).

3.3. Oxidation reaction energy

Oxidation of Pu_2O_3 via the reaction

$$Pu_2O_3 + \frac{1}{2}O_2 \rightarrow 2PuO_2 \qquad (2)$$

leads to the formation of stoichiometric PuO_2. The dependence of the transformation reaction energy on U is presented in Fig.9. One can see that both the LDA and the GGA show the same dependences of reaction energy on the on-site Coulomb interaction. That is, at small values of U which correspond to the metallic ground state for both PuO_2 and Pu_2O_3, the reaction energy is independent of U. Above the metallic-insulating transition, our calculated reaction energy decreases linearly with U increasing. The reason for this behaviour is that a high value of U favours localization and thus facilitates the transition. The density functional theory is known to overestimate the binding energy of O_2 and this should result in the underestimation of the present reaction energy via the E_{O_2} term. Consequently we cannot expect a perfect agreement with experimental result for the present reaction energy. However, this error is independent of

any condition in the plutonium oxide and thus can be remedied by shifting the energy of O_2 so as to give the experimental binding energy. In the LDA the O_2 binding energy is overestimated by 1.2 eV/0.5 O_2 and in the GGA the corresponding figure is 0.8 eV/0.5 O_2. The GGA always predicts a lower value of the reaction energy, as seen from Fig.9.

4. Conclusions

We have studied the structural, electronic, and thermodynamic properties of PuO_2 and Pu_2O_3 within the LDA+U and GGA+U formalisms. From the study of the lattice parameter of PuO_2 we find that the experimental data of a_0 can be well fitted by the GGA using $U = 3$ eV, while the LDA always gives an underestimation in the whole range of U. Thus we conclude that the GGA scheme reveals acceptable agreement with experiment than the LDA; this is partly due to the more accurate treatment of correlation effects within the GGA potential. It has also been shown in this paper that the incorrect metallic ground state at pure LDA or GGA ($U = 0$) for both PuO_2 and Pu_2O_3 can be readily corrected by the systematic inclusion of non-zero U, which forces the Pu 5f band to gradually split at the Fermi energy and thus drives the metallic-insulating transition. The band gaps and the position of the Pu 5f band relative to O(2p) band for PuO_2 and Pu_2O_3 have been shown as a function of U. The oxidation reaction Pu_2O_3+0.5O_2 →2PuO_2 has also been studied by systematically calculating the reaction energy as a function of U. Our results show that the oxidation process of the Pu_2O_3 is an exothermic reaction, which is mostly responsible for the experimentally observed[37] plutonium pyrophoricity at 150–200°C. Also we have shown that above the metallic-insulating transition, the reaction energies decrease with U increasing for the LDA and the GGA schemes. We expect these calculated results to be useful for the future studies on the surface oxidation and corrosion of metallic plutonium.

References

[1] Haschke J M 2000 *Los Alamos Science* **26** 253
[2] Haschke J M, Allen T H and Morales L A 2000 *Science* **287** 285
[3] Anisimov V I, Zaanen J and Anderson O K 1991 *Phys. Rev.* B **44** 943
[4] Anisimov V I, Solovyev I V, Korotin M A, Czyżyk M T and Sawatzky G A 1993 *Phys. Rev.* B **48** 16929
[5] Solovyev I V, Dederichs P H and Anisimov V I 1994 *Phys. Rev.* B **50** 16861
[6] Savrasov S Y and Kotliar G 2000 *Phys. Rev. Lett.* **84** 3670
[7] Chen L J 2006 *Chin. Phys.* **15** 798
[8] Jin Y J, Lin J B and Lee J I 2007 *Chin. Phys.* **16** 506
[9] Zhu Z Y, Wang B, Wang H, Zheng Y and Li Q K 2007 *Chin. Phys.* **16** 1780
[10] Song H Z, Zhang P and Zhao X G 2006 *Acta Phys. Sin.* **55** 6205 (in Chinese)
[11] Song H Z, Zhang P and Zhao X G 2007 *Acta Phys. Sin.* **56** 456 (in Chinese)
[12] Sun B, Liu S J and Zhu W J 2006 *Acta Phys. Sin.* **55** 6589 (in Chinese)
[13] Sun B, Liu S J, Duan S Q and Zhu W J 2007 *Acta Phys. Sin.* **56** 1598 (in Chinese)
[14] Qiu A N, Wu J S and Zhang L T 2007 *Acta Phys. Sin.* **56** 4891 (in Chinese)
[15] Ding S, Fan G T, Li S T and Xiao B 2007 *Acta Phys. Sin.* **56** 4062 (in Chinese)
[16] Deng H Q, Hu W Y, Li W X and Zeng Z H 2006 *Acta Phys. Sin.* **55** 3157 (in Chinese)
[17] Deng S H, Lü G H, Wang T M, Wang T M and Zhang Y 2006 *Acta Phys. Sin.* **55** 2901 (in Chinese)
[18] Chen D, Gao T, Wang C L and Yu B H 2007 *Chin. Phys.* **16** 2056
[19] Cai W, Tan C L and Tian X H 2006 *Chin. Phys.* **15** 2718
[20] Li Z L, Luo Y, Wang C K and Xue Q K 2005 *Chin. Phys.* **14** 1036
[21] Hao I A and Zheng H P 2005 *Chin. Phys.* **14** 529
[22] Loschen C, Loschen J, Neyman K M and Illas F 2007 *Phys. Rev.* B **75** 035115
[23] Andersson D A, Simak S I, Johansson B, Abrikosov I A and Skorodumova N V 2007 *Phys. Rev.* B **75** 035109
[24] Dudarev S L, Dudarev G A, Savrasov S Y, Humphreys C J and Sutton A P 1998 *Phys. Rev.* B **57** 1505
[25] Blöchl P E 1994 *Phys. Rev.* B **50** 17953
[26] Kresse G and Hafner J 1993 *Phys. Rev.* B **48** 13115
[27] Kresse G and Furthmüller J 1996 *Comput. Mater. Sci.* **6** 15
[28] Kresse G and Furthmüller J 1996 *Phys. Rev.* B **54** 11169
[29] Kresse G and Joubert D 1999 *Phys. Rev.* B **59** 1758
[30] Perdew J P, Chevary J A Chevary, Vosko S H, Jackson K A, Pederson M R, Singh D J and Fiolhais C 1992 *Phys. Rev.* B **46** 6671
[31] Monkhorst H J and Pack J D 1972 *Phys. Rev.* B **13** 5188
[32] Blöchl P E, Jepsen O and Andersen O K 1994 *Phys. Rev.* B **49** 16223
[33] Haire R G and Haschke J M 2001 *MRSBull* p689
[34] Birch F 1938 *J. Appl. Phys.* **9** 279
[35] Birch F 1947 *Phys. Rev.* **71** 809
[36] http://cms.mpi.univie.ac.at/vasp/vasp/node196.html.
[37] Martz J C, Haschke J M and Stakebake J L 1994 *J. Nuclear Materials* **210** 130